Article

JOURNAL OF COMPOSITE MATERIALS

Journal of Composite Materials
0(0) 1–10

DOI: 10.1177/0021998317696137
journals.sagepub.com/home/jcm

SAGE

Thermal conductivity of epoxy composites filled by thermally reduced graphite oxide with different reduction degree

Yingying Sun[1], Lin Chen[1], Jun Lin[2], Peng Cui[2], Meicheng Li[2] and Xiaoze Du[1]

Abstract

A series of selectively reduced graphite oxide was prepared by thermal reduction of graphite oxide at different annealing temperatures and used as fillers to enhance thermal conductivity of epoxy composites. The reduction degree of selectively reduced graphite oxide increases with annealing temperature changing from 600°C to 1000°C. The out-of-plane thermal conductivity (K_o) of selectively reduced graphite oxide/epoxy composites is remarkably higher than that of graphite oxide/epoxy. For the selectively reduced graphite oxide obtained at 1000°C, K_o reaches 0.674 W/m·K when filler content is 5.4 wt%, which is 450% of pure epoxy. The enhanced K_o can be attributed to the better dispersion of selectively reduced graphite oxide in epoxy and their edges overlap to form effective thermal conductive paths in epoxy matrix. However, the achieved thermal conductivity enhancement is still comparatively lower than that of selectively reduced graphite oxide with higher reduction degree, since the interfacial bonding strength between selectively reduced graphite oxide and epoxy decreases when reduction degree of selectively reduced graphite oxide flakes becomes higher.

Keywords

Polymer composites, thermal properties, interface, thermal analysis

Introduction

A raft of recent research has been performed to improve the thermal conductivity of epoxy composites by introducing thermally conducive fillers into the epoxy matrix, such as carbon nanotubes, carbon fiber, aluminum oxide, boron nitride, and graphene.[1–4] Among these fillers, graphene can significantly improve thermal conductivity of composites at extremely small loading due to its high thermal conductivity[5,6] and atomically thin sheet structure.[7] However, the thermal conductivity of graphene/epoxy composites is still not high enough to meet the application needs.[8–10] According to the literature,[10–12] the main ways to improve the thermal conductivity of graphene/epoxy composites are improving the quality of graphene, improving its dispersion in epoxy matrix, and enhancing the interfacial bonding strength between fillers and matrix. Fu et al.[13] filled epoxy adhesive with few-layer modified graphene flakes, which were prepared by re-expansion and thermal exfoliation of graphite nanoflake, and the thermal conductivity of composites reached 4.01 W/m·K at 10.10 wt% filler content. Wang et al.[11] found that under good mixture condition, thermal conductivity of epoxy composites with 8 wt% commercial graphene nanoplatelets could reach 1.181 W/m·K, which was 627% enhancement of pure epoxy. Chatterjee et al.[14] used amine functionalized

[1]Key Laboratory of Condition Monitoring and Control for Power Plant Equipment, North China Electric Power University, China
[2]School of Renewable Energy, North China Electric Power University, China

Corresponding author:
Lin Chen, Key Laboratory of Condition Monitoring and Control for Power Plant Equipment, North China Electric Power University, Beijing, 102206, China.
Email: chenlin@ncepu.edu.cn

expanded graphene nanoplatelets to improve the thermal properties of epoxy composites and observed that the thermal conductivity of composites reached 136% of epoxy resin at only 2 wt% filler content.

Until now, a variety of methods has been reported to prepare high quality graphene, which include mechanical cleavage method,[5] epitaxial growth on SiC,[15] reduction/exfoliation of graphite oxide (GO),[16] unzipping carbon nanotubes,[17] and chemical vapor deposition (CVD).[18] Among these methods, reduction/exfoliation of GO are more suitable for polymer composite applications[19,20] because the products, reduced GO (r-GO) flakes, are modified graphene flakes.[21] Small amount of oxygen-containing functional groups on the surface of r-GO flakes are beneficial to their dispersion in polymer matrix and can strengthen the bonding force between fillers and matrix.[22] Then the polymer composites with high thermal conductivity and better mechanical properties can be produced, which have great potential applications in thermal management of electronic packaging,[2] plastic heat exchanger,[23] thermal interfacial materials,[24] and so on. But too many functional groups decrease the thermal conductivity of r-GO, which is harmful for improving the thermal conductivity of polymer composites.[25] Therefore, to improve the thermal properties of polymer composites, the quantity of functional groups should be appropriate. Until now, the amount of oxygen can be controlled by experimental conditions.[26] The amount of oxygen here corresponds to the reduction level of GO to modified graphene flakes, which is named as reduction degree in this article. Thermal reduction and chemical reduction of GO are both simple and stable methods to produce modified graphene flakes in a large scale.[27,28] It has been reported that the annealing temperature greatly influenced the reduction degree of GO, and then influenced the thermal conductivity of r-GO flakes.[25] Therefore, thermal reduction of GO is an interesting choice to do research on the influence of GO's reduction degree to the thermal conductivity of r-GO/polymer composites.

In this article, selectively reduced graphite oxide (SRGO) with different reduction degree was obtained by thermal reduction/exfoliation[29] at temperatures ranging from 600°C to 1000°C. Then the effect of SRGO's reduction degree on the thermal conductivity of SRGO/epoxy composites is systematically investigated. To explain the variation trend of thermal conductivity, further experimental studies on the quality of SRGO flakes, dispersion of SRGO in epoxy matrix, the reaction between SRGO and epoxy matrix, and the interfacial bonding strength between SRGO and epoxy matrix were discussed.

Experimental and sample characterization

Synthesis of GO

Synthetic graphite powder with diameter less than 0.5 mm was used as raw material for the preparation of GO. In this study, GO was synthesized according to a modified Hummer's method,[30,31] which took place in a 1000 ml three-necked round-bottomed flask. First, under the circumstance of 0°C ice-salt bath, graphite power (3 g) was dispersed in the solution of concentrated H_2SO_4 (98%, 100 ml), and then $NaNO_3$ (3 g) and $KMnO_4$ (12 g) were added to the mixture, stirring for 2 h at 300 rpm. Second, the mixture was heated to 35°C, and kept stirring for 40 min. Deionized water (138 ml) was slowly dropped into the reagent under the circumstance of 0°C ice-salt bath. Third, the flask was transferred into 98°C thermostatic bath immediately, kept stirring for 20 min, and cooled down naturally to 50°C. Then the reagent was diluted by 45°C deionized water (350 ml), in which H_2O_2 (70 ml) was slowly added. After stirring for 1 h, the reagent was successively washed with the 1:10 HCl solution (330 ml), methanol (100 ml), and deionized water (100 ml) through suction filtration, until sulfate ion and mental ion were totally filtered out, and the pH was neutral. Finally, the remained GO was dried at 45°C in vacuum oven (DZF6050, Jinghong, China) for 24 h.

Selective thermal reduction of GO

The GO was thermally reduced in a horizontal tube furnace (STF-1200X, China). Initially, five samples (1 g for each sample) were degassed under a nitrogen gas flow of 80 ml/min at room temperature for 20 min. Then the samples were heated to 400°C at the rate of 5°C/min, and kept at 400°C for 30 min. After that, the five samples were heated from 400°C to 600°C, 700°C, 800°C, 900°C, and 1000°C, respectively, at the rate of 5°C/min. At each terminal temperature, the sample was kept for 30 min. Finally, the samples were naturally cooled to room temperature. These samples prepared above were named as SRGO600, SRGO700, SRGO800, SRGO900, and SRGO1000, respectively.

Preparation of SRGO/epoxy composites

Since the preparation processes are similar, the procedure for preparing 0.5 wt% SRGO/epoxy composites was taken as an example. First, SRGO was ultrasonically dispersed in acetone for 30 min (sonic power 80 W) and then blended with the epoxy resin (E-51, Sanmu Corporation, China) and curing agent (2,3,6-tetrahydro-3-methylphthalic anhydride) by magnetically stirring for 1 h at 60°C. The mass fraction ratio of SRGO: epoxy resin: curing

agent is 1:100:85. Second, the mixture was ultrasonically dispersed for 30 min at 60°C. Third, the accelerator, 2,4,6-tris(dimethylaminomethyl)phenol, was added into the liquid mixture according to the mass ratio 1:100 to epoxy resin, and the mixture was magnetically stirred for 30 min at 60°C. Then the mixture was degassed for 1 h to remove bubbles at 80°C in vacuum oven. After that, the mixture was transferred to a polytetrafluoroethene (PTFE) mold (diameter 12.7 mm, thickness 2 mm) and cured at 100°C for 4 h and 150°C for 4 h. Finally, the cured sample was naturally cooled to room temperature. The composites prepared were named as SRGO/epoxy-0.5. Through the same procedure, the samples of SRGO/epoxy-1.0, SRGO/epoxy-2.7, and SRGO/epoxy-5.4 were obtained.

Characterization of samples

To verify the quality of SRGO, samples were characterized by X-ray diffractometer (XRD, Cu/K-α1 radiation, Bruker D8 Advance, German) under a power supply of 40 kV and 40 mA with a scanning speed of 5°/min from 5° to 50°, Raman spectrophotometer (LabRAM Aramis, 633 nm helium-neon laser, France) recorded from 200 to 3700 cm^{-1}, X-ray photoelectron spectrometer (XPS, K-α1, ESCALAB 250, USA) performed under 200 eV for survey and 30 eV for high resolution scans, and transmission electron microscope (TEM, JEM-2100 LaB_6, Japan) at 160 keV.

The dispersing morphologies and interfacial properties of SRGO flakes in epoxy matrix were characterized by cold field emission gun scanning electron microscope (SEM, SU8010, Japan) at 5.0 kV and TEM (FEI Tecnai G^2 F20, Netherlands) at 160 keV. Fourier transform infrared spectrometer (FT-IR, NICOLET iS10, USA) was performed to identify the functional groups of SRGOs/epoxy composites. Thermal diffusivity (α) was measured on a laser flash thermal analyzer (NETZSCH-LFA 447 NanoFlash, German) at 30°C. Specific heat capacity (C_P) was measured on a differential scanning calorimeter instrument (NETZSCH-DSC 404, German) under argon atmosphere with a heating rate of 10°C/min. The density (ρ) was measured by Buoyancy Method. Then the thermal conductivity, K, was obtained by,

$$K = \alpha \cdot C_P \cdot \rho \tag{1}$$

Results and discussion

Reduction degree of SRGO and its influence on microstructure

The amount of oxygen on the surface of SRGO flakes was measured by XPS analysis, and the results are listed in Table 1. It is found that more oxygen-containing functional groups are decomposed when the annealing temperature increases, i.e. the reduction degree of SRGO increases with the annealing temperature increasing from 600°C to 1000°C.

Table 1. XPS analysis of GO and SRGO elemental composition.

Sample	C (%)	O (%)	C/O
GO	79.96	20.04	3.99
SRGO600	85.64	14.36	5.96
SRGO700	86.21	13.79	6.25
SRGO800	88.44	11.56	7.65
SRGO900	90.80	9.20	9.87
SRGO1000	93.57	6.43	14.55

The variation of microstructure with reduction degree of SRGO flakes was characterized by XRD, Raman, and TEM. As shown in XRD patterns of Figure 1(a), the sharp peak of GO around 11° corresponds to the (001) plane. The peak around 26.3° of graphite corresponds to the (002) plane. The disappearance of (001) peak of SRGO demonstrates the successful exfoliation of GO, while the existence of (002) peak shows that the prepared GO and SRGO flakes are multilayer. According to Scherrer Equation and Bragg Equation,[32,33] the crystallite size, L, and interlaminar distance, d_{002}, can be respectively calculated. The number of layers, n, is roughly estimated by

$$n = \frac{L}{d_{002}} + 1 \tag{2}$$

The values of d_{002}, L and n are listed in Table 2, in which d_{002} and n of SRGO are similar. And the number of layers n changes from 24 to 26. The layer structure of SRGO flakes and their shapes can also be seen from TEM pictures of SRGO flakes. It is confirmed that the number of layers of SRGO flakes with different reduction degree and their shapes are similar. This is because the GO was synthesized by the same method, and the oxygen-containing groups were inserted into the similar layers of the graphite powders. When the oxygen-containing groups decomposed at quite high temperature, the GO expanded in these similar layers. Taking the TEM pictures of SRGO800 flakes as an example, Figure 1(c) demonstrates that the number of layers n changes between 20 and 30, and Figure 1(d) shows that the individual SRGO flake presents to be transparent and silk-like, possessing a large aspect ratio, which is beneficial to the overlap of the SRGO flakes in epoxy resin. As demonstrated in Raman spectrum of Figure 1(b), the prepared SRGO flakes are defected in structure, and the defect degree of SRGO increases with

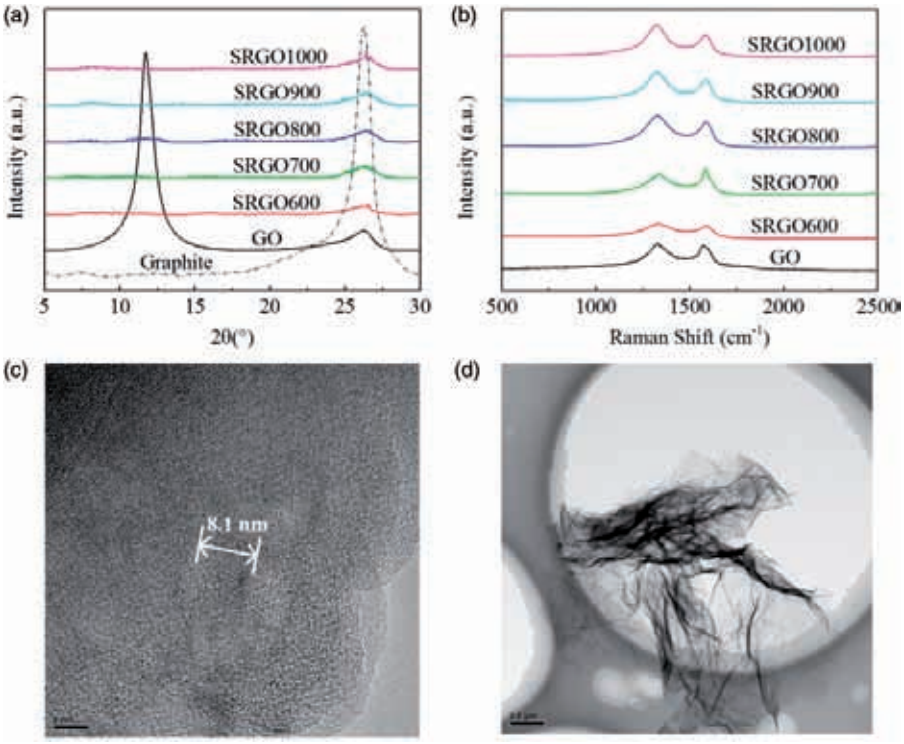

Figure 1. Structural characterization of fillers. (a) XRD patterns, (b) Raman spectra, (c) high resolution TEM images of SRGO800, and (d) TEM images of SRGO800.

Table 2. XRD analysis of graphite, GO, and SRGO, the interlaminar distance, crystallite size, and estimated number of layers.

Sample	d_{002} (nm)	L (nm)	n
Graphite	0.336	28.000	84
GO	0.339	7.900	24
SRGO600	0.335	8.500	26
SRGO700	0.337	8.000	25
SRGO800	0.335	8.000	25
SRGO900	0.336	8.100	25
SRGO1000	0.336	8.500	26

the increase of reduction degree owing to the decomposition of oxygen-containing groups.[26]

Out-of-plane thermal conductivity of SRGO/epoxy composites

The out-of-plane thermal conductivity, K_o, of GO/epoxy and SRGO/epoxy composites is shown in Figure 2(a). Apparently when the filler content increasing, the K_o of composites increases accordingly, and K_o of SRGO/epoxy composites is higher than that of GO/epoxy composites. When the filler content is larger than 1.0 wt%, K_o of SRGO/epoxy composites is enhanced with the increasing annealing temperature of SRGO, i.e. K_o of SRGO/epoxy composites increases with the rising reduction degree of SRGO. The maximum K_o value of SRGO/epoxy-1.0, SRGO/epoxy-2.7, and SRGO/epoxy-5.4, respectively, reaches 0.259, 0.409, and 0.674 W/m·K, which is 173%, 273%, and 450% times of pure epoxy. It is notable that the superiority of increasing reduction degree of SRGO becomes more evident with the increase of filler content. As can be seen from Figure 2(b), the K_o ratio of SRGO1000/epoxy to GO/epoxy, $K_{o\text{-SRGO1000/epoxy}}/K_{o\text{-GO/epoxy}}$, increase from 106% to 349%, and the variation trend is almost linear. According to the previous literature,[25] thermal conductivity of SRGO increases with the increase of annealing temperature, and there is a 141 times increase when the annealing temperature changes from 900°C to 1000°C. However, the dramatic change of thermal conductivity does not occur when SRGO flakes are compounded with epoxy resin. The main reason might be the thermal resistance of interface layer between SRGO flakes and epoxy matrix, which will be discussed in the next section. Besides, K_o of SRGO/epoxy-0.5 composites changes very little with reduction degree. This is mainly because the SRGO flakes are so few that they are randomly dispersed in the matrix and isolated from each other, and consequently the thermal conductivity of epoxy composites changes very little with the thermal property of fillers and interface layer.

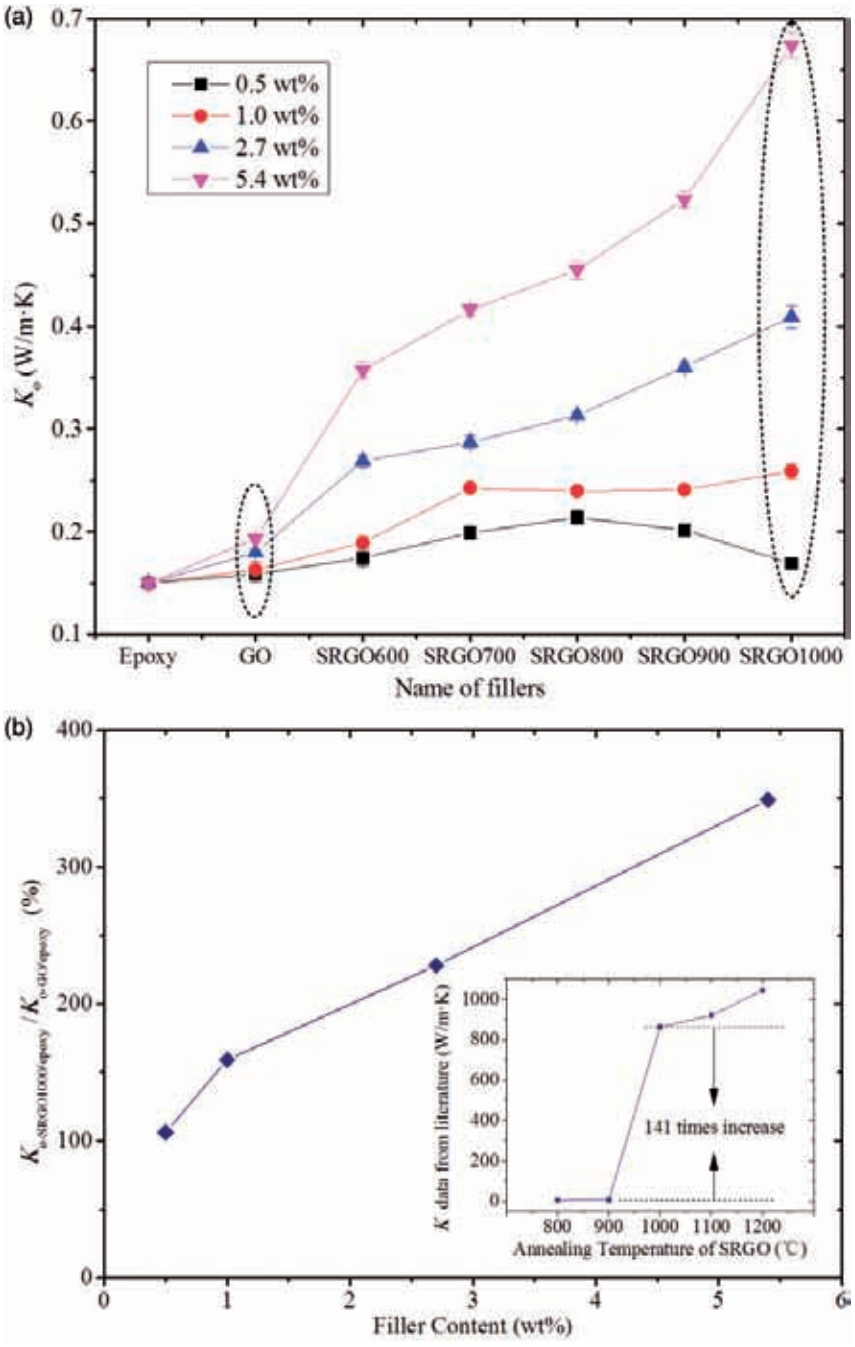

Figure 2. Experimental results of out-of-plane thermal conductivity of epoxy composites. (a) Detailed data, (b) variation trend of $K_{o\text{-SRGO1000/epoxy}}/K_{o\text{-GO/epoxy}}$ (i.e. out-of-plane thermal conductivity ratio of SRGO1000/epoxy composites and GO/epoxy composites) with filler content. The thermal conductivity data of Song's literature[25] are shown in the inset graph of (b) and when the annealing temperature changes from 900°C to 1000°C, thermal conductivity of SRGO flakes dramatically increases by 141 times.

Explanation of the growth trends of K_o

Physical property of interface layer between SRGO flakes and epoxy matrix. The interaction between the functional groups of SRGO flakes and epoxy was characterized by FT-IR method. As demonstrated in FT-IR spectra of Figure 3(a), the peak around 827 cm^{-1} corresponds to stretching C–O–C of oxirane group, the peak around 913 cm^{-1} represents the stretching C–O of oxirane group, the peak around 1036 cm^{-1} corresponds to stretching C–O–C of ethers and the peaks from 1506 cm^{-1} to 1608 cm^{-1} represent the stretching C–C

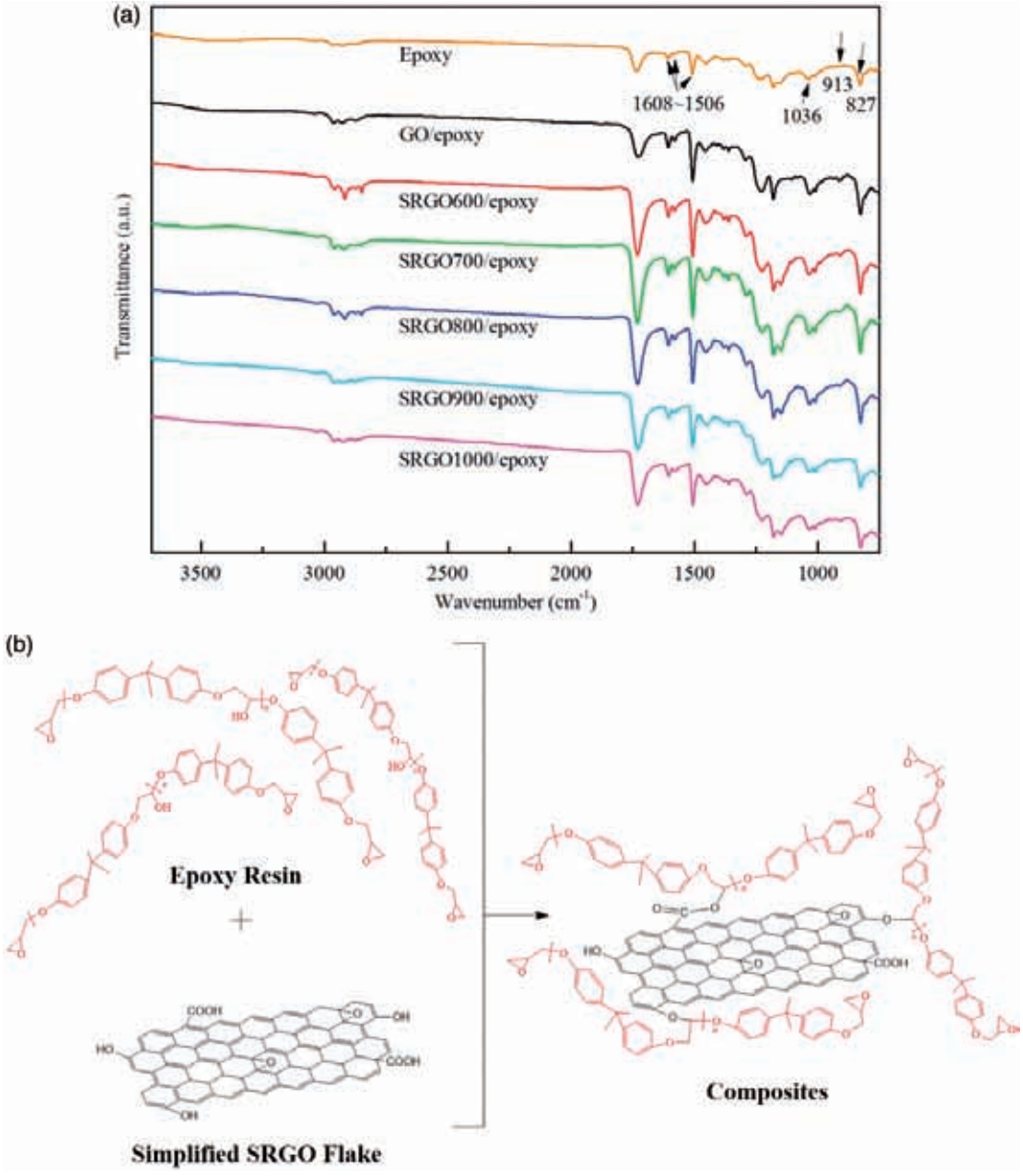

Figure 3. The interaction between SRGO flakes and epoxy resin. (a) FT-IR spectra of pure epoxy and epoxy composites (filler content = 5.4 wt%). (b) The chemical diagram of reaction between the functional groups of SRGO flakes and epoxy resin, in which SRGO flakes are simplified as one layer.

and stretching C = C of aromatic rings. It is found that the relative content of C–O of oxirane group, C–O–C of oxirane group, and C–O–C of ethers in epoxy composites is larger than that in pure epoxy, and it reaches maximum in GO/epoxy composites. This indicates that the hydroxyl and carboxyl groups carried by fillers react with the hydroxyl of epoxy resin. As shown in Figure 3(b), partial hydroxyl and hydrogen in epoxy resin are removal, and some new C–O–C of oxirane groups are brought in by SRGO. Meanwhile, as a reaction product, some C–O–C of ethers are introduced.

The SEM images of GO/epoxy-5.4 and SRGO/epoxy-5.4 composites are shown in Figure 4, from which the dispersion of SRGO flakes and physical property of interface layer can be analyzed. When the reduction degree of SRGO increases, the interfacial gaps between SRGO and epoxy matrix become larger, which indicates that the interfacial bonding strength between SRGO flakes and epoxy matrix decreases. This is mainly attributed to the decomposition of oxygen-containing functional groups. The oxygen-containing functional groups could interact with epoxy resin, and then enhance the interfacial bonding force

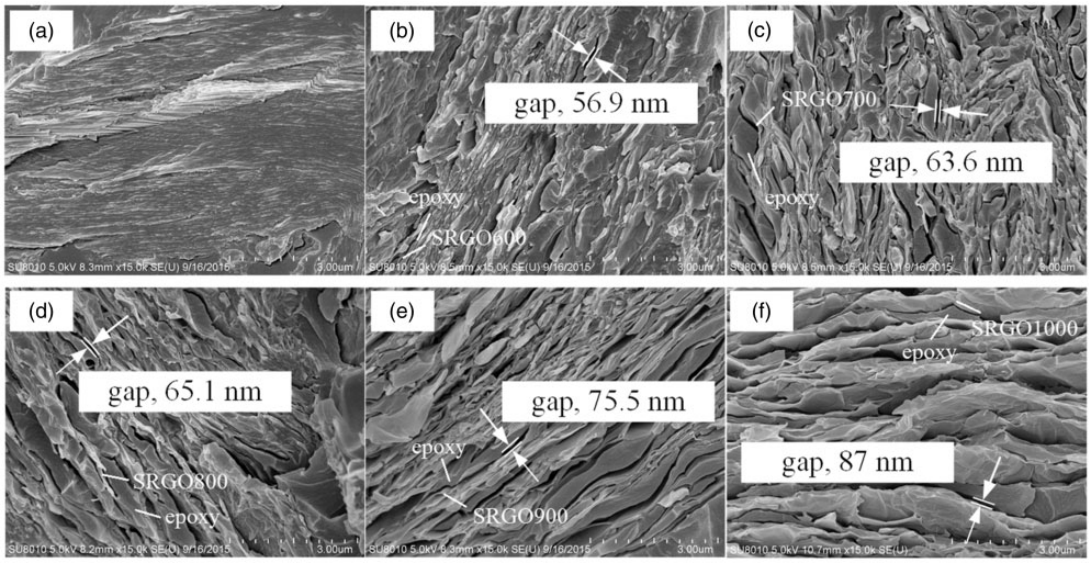

Figure 4. SEM images of epoxy composites (filler content = 5.4 wt%). (a) GO/epoxy, (b) SRGO600/epoxy, (c) SRGO700/epoxy, (d) SRGO800/epoxy, (e) SRGO900/epoxy, and (f) SRGO1000/epoxy.

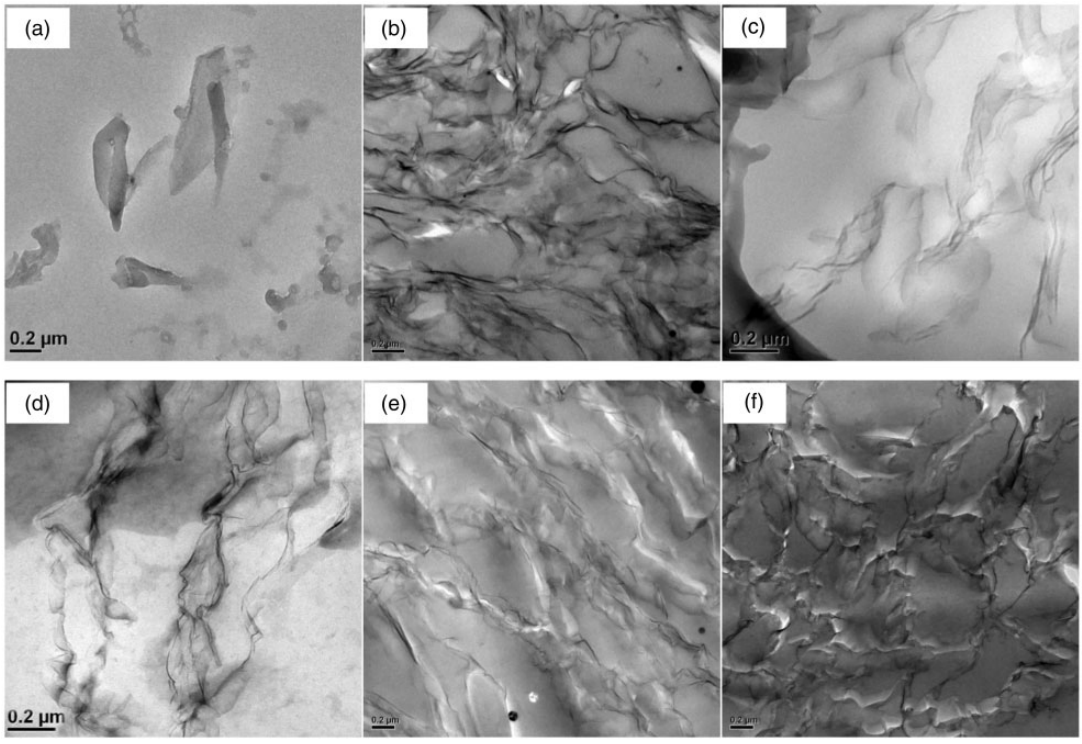

Figure 5. TEM images of epoxy composites (filler content = 5.4 wt%). (a) GO/epoxy, (b) SRGO600/epoxy, (c) SRGO700/epoxy, (d) SRGO800/epoxy, (e) SRGO900/epoxy, and (f) SRGO1000/epoxy.

and compactness between SRGO flakes and epoxy matrix.[34] Therefore, less oxygen-containing functional groups would result in larger interfacial gaps. In addition, the interfacial bonding force and compactness greatly influence the heat transfer in interface layer. When the interfacial bonding force is weaker and the compactness is smaller, the diffuse acoustic mismatch effect[35,36] strengthens and heat transfer of interface

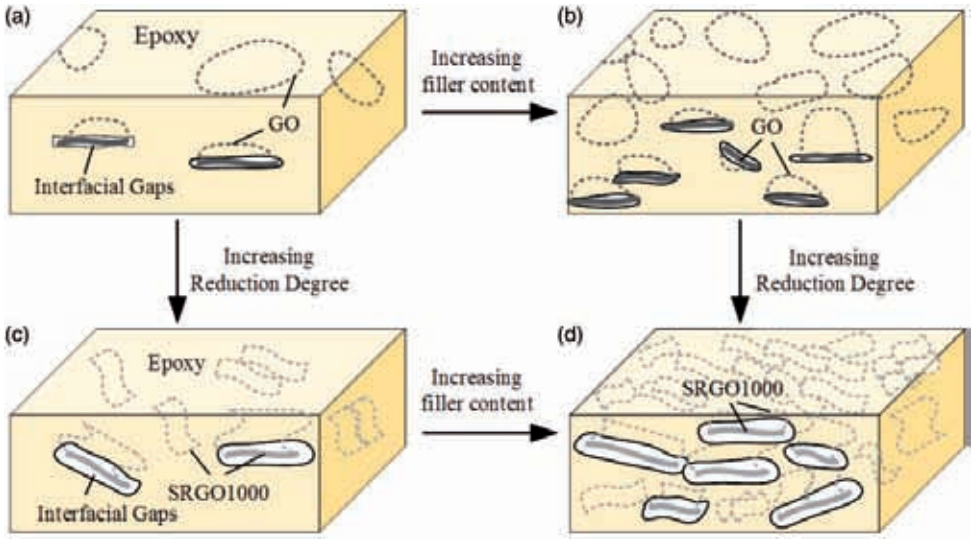

Figure 6. The variation of three-dimensional models of epoxy composites with filler content and reduction degree of fillers. (a) Model of GO/epoxy-0.5 composites, (b) model of GO/epoxy-5.4 composites, (c) model of SRGO1000/epoxy-0.5 composites, and (d) model of SRGO1000/epoxy-5.4 composites. In these models, fillers in the internal composites are represented by dotted lines, while fillers truncated by surfaces are represented by thick solid lines and dotted lines. The thick solid lines are the intersections of fillers and surfaces, which can be observed from outside. And the white spaces around the thick solid lines are interfacial gaps.

caused by lattice vibration is less effective, which means the interfacial thermal resistance increases.[34,37,38]

Dispersion of SRGO flakes in the epoxy matrix. Besides the physical property of interface layer, the dispersion of SRGO flakes in epoxy matrix are also discussed. Figure 5 shows the TEM images of GO/epoxy-5.4 and SRGO/epoxy-5.4 composites. It can be found that when the weight fraction of filler reaches 5.4 wt%, the GO particles are still isolated dispersed in epoxy matrix owing to its granular shape, while the edges of SRGO flakes overlap, forming effective thermal conductive paths in the epoxy matrix. This formation of thermal conductive path is beneficial for improving the thermal conductivity of epoxy composites[39] and is an important reason for the enhanced thermal conductivity of the SRGO/epoxy composites as compared to that of the GO/epoxy composites. At the same filler content of 5.4 wt%, the distributions of SRGO flakes with different reduction degree are different, but the SRGO flakes all overlap in the matrix. This is mainly due to the large aspect ratio and flexible shape of SRGO flakes. Then the effect of distribution difference caused by SRGO flakes is covered up.

Three-dimensional models of SRGO/epoxy composites. To explain the variation trend of out-of-plane thermal conductivity of composites, the thermal transfer models of epoxy composites including GO or SRGO flakes, epoxy matrix, and interfacial gaps are set up according to the results of XPS analysis, FT-IR spectra, SEM images, and TEM images. As shown in Figure 6, at 0.5 wt% filler content, GO and SRGO flakes are all isolated in epoxy matrix, and with the increase of reduction degree, the size of interfacial gaps between SRGO flakes and epoxy matrix increases. So the thermal conductivity of SRGO1000/epoxy-0.5 composites is closed to that of GO/epoxy-0.5 composites. When filler content becomes larger, the GO particles are still isolated in epoxy resin, while the edges of SRGO flakes become overlapped. So the thermal conductivity of SRGO1000/epoxy-5.4 composites is much higher than that of GO/epoxy-5.4 composites. As shown in Figure 2(b), the thermal conductivity of SRGO flakes increases 141 times when the annealing temperature increases from 900°C to 1000°C. If the thermal conductivity of the interface layer is the same, there will be a sharp improvement in the thermal conductivity of SRGO/epoxy composites when the fillers change from SRGO900 to SRGO1000. However, with the increase of reduction degree, the interfacial bonding strength between SRGO flakes and epoxy resin decreases and the interfacial gaps increase, and then the heat transfer efficiency of the interface layer decreases. So the dramatic thermal conductivity increase of SRGO flakes changing from SRGO900 to SRGO1000 does not occur in the thermal conductivity of their epoxy composites as shown in Figure 2(a).

Conclusions

Thermally selective reduction/exfoliation of GO was conducted under different annealing temperature from 600°C to 1000°C. Then SRGO flakes with different

reduction degree were used to enhance thermal conductivity of epoxy composites. And the following conclusions were obtained.

1. Compared with GO particles, SRGO flakes present a better dispersion morphology in the epoxy matrix. When the weight fraction of SRGO flakes reaches 5.4%, the edges of SRGO flakes overlap, forming an effective thermal conductive path in epoxy composites.
2. The out-of-plane thermal conductivity of SRGO/epoxy composites becomes larger when the reduction degree of SRGO flakes increase. However, with higher reduction degree, the content of oxygen-containing functional groups connecting SRGO flakes and epoxy matrix decreases, and the interfacial gaps between SRGO flakes and epoxy resin increase. So the thermal conductivity of SRGO/epoxy composites does not change dramatically with that of SRGO flakes. To explain the variation trend of thermal conductivity of composites, thermal transfer models of epoxy composites changing with the increase of filler content and reduction degree are built in this article.
3. SRGO flakes with high reduction degree is better suitable as the filler of polymer composites and are expected to improve the thermal conductivity of SRGO/polymer composites substantially at low filler content. When taking SRGO1000 as filler, K_o of SRGO/epoxy-1.0, SRGO/epoxy-2.7, and SRGO/epoxy-5.4 composites, respectively, can reach 0.259, 0.409, and 0.674 W/m·K, which is 173%, 273%, and 450% times of the pure epoxy resin.

Highlights

- SRGO with higher reduction degree better enhances thermal conductivity of composites.
- Interfacial gaps between SRGO and epoxy increases when reduction degree increases.
- Compared with GO particles, SRGO flakes present a more effective dispersion in epoxy.
- Composite models changing with reduction degree of SRGO and filler content are built.

Declaration of Conflicting Interests

The author(s) declared no potential conflicts of interest with respect to the research, authorship, and/or publication of this article.

Funding

The author(s) disclosed receipt of the following financial support for the research, authorship, and/or publication of this article: National Natural Science Foundation of China (51406052), National Basic Research Program of China (973 Program) (2015CB251503), and Fundamental Research Funds for the Central Universities (2015XS85, 2016YQ03).

References

1. Yu J, Huang X, Wang L, et al. Preparation of hyperbranched aromatic polyamide grafted nanoparticles for thermal properties reinforcement of epoxy composites. *Polym Chem* 2011; 2: 1380–1388.
2. Yu A, Ramesh P, Sun X, et al. Enhanced thermal conductivity in a hybrid graphite nanoplatelet - Carbon nanotube filler for epoxy composites. *Adv Mater* 2008; 20: 4740–4744.
3. Kim K and Kim J. Fabrication of thermally conductive composite with surface modified boron nitride by epoxy wetting method. *Ceram Int* 2014; 40: 5181–5189.
4. Yuan C, Duan B, Li L, et al. Thermal conductivity of polymer-based composites with magnetic aligned hexagonal boron nitride platelets. *ACS Appl Mater Interf* 2015; 7: 13000–13006.
5. Novoselov KS, Geim AK, Morozov SV, et al. Electric field effect in atomically thin carbon films. *Science* 2004; 306: 666–669.
6. Balandin AA, Ghosh S, Bao W, et al. Superior thermal conductivity of single-layer graphene. *Nano Lett* 2008; 8: 902–907.
7. Yao W-J and Cao B-Y. Thermal wave propagation in graphene studied by molecular dynamics simulations. *Chin Sci Bull* 2014; 59: 3495–3503.
8. Zeng C, Lu S, Song L, et al. Enhanced thermal properties in a hybrid graphene–alumina filler for epoxy composites. *RSC Adv* 2015; 5: 35773–35782.
9. Chen L, Sun Y-Y, Lin J, et al. Modeling and analysis of synergistic effect in thermal conductivity enhancement of polymer composites with hybrid filler. *Int J Heat Mass Transf* 2015; 81: 457–464.
10. Wan Y-J, Tang L-C, Gong L-X, et al. Grafting of epoxy chains onto graphene oxide for epoxy composites with improved mechanical and thermal properties. *Carbon* 2014; 69: 467–480.
11. Wang Y, Yu J, Dai W, et al. Enhanced thermal and electrical properties of epoxy composites reinforced with graphene nanoplatelets. *Polym Compos* 2015; 36: 556–565.
12. Shtein M, Nadiv R, Buzaglo M, et al. Thermally conductive graphene-polymer composites: size, percolation, and synergy effects. *Chem Mater* 2015; 27: 2100–2106.
13. Fu Y-X, He Z-X, Mo D-C, et al. Thermal conductivity enhancement of epoxy adhesive using graphene sheets as additives. *Int J Therm Sci* 2014; 86: 276–283.
14. Chatterjee S, Wang JW, Kuo WS, et al. Mechanical reinforcement and thermal conductivity in expanded graphene nanoplatelets reinforced epoxy composites. *Chem Phys Lett* 2012; 531: 6–10.
15. Berger C, Song Z, Li T, et al. First, ultrathin epitaxial graphite layers: 2D electron gas properties and a route towards graphene based nanoelectronics. *J Phys Chem B* 2004; 108: 19912–19916.

16. Stankovich S. Stable aqueous dispersions of graphitic nanoplatelets via the reduction of exfoliated graphite oxide in the presence of poly(sodium 4-styrenesulfonate). *J Mater Chem* 2006; 16: 155–158.
17. Kosynkin DV, Higginbotham AL, Alexander S, et al. Longitudinal unzipping of carbon nanotubes to form graphene nanoribbons. *Nature* 2009; 458: 872–876.
18. Wang X, You H, Liu F, et al. Large scale synthesis of few-layered graphene using CVD. *Chem Vapor Depos* 2009; 15: 53–56.
19. Kim H, Abdala AA and Macosko CW. Graphene/polymer nanocomposites. *Macromolecules* 2010; 43: 6515–6530.
20. Yu W, Xie H, Chen L, et al. Graphene based silicone thermal greases. *Phys Lett A* 2014; 378: 207–211.
21. Lonkar SP, Deshmukh YS and Abdala AA. Recent advances in chemical modifications of graphene. *Nano Res* 2014; 8: 1039–1074.
22. Fang M, Wang K, Lu H, et al. Covalent polymer functionalization of graphene nanosheets and mechanical properties of composites. *J Mater Chem* 2009; 19: 7098–7105.
23. Chen L, Li Z and Guo ZY. Experimental investigation of plastic finned-tube heat exchangers, with emphasis on material thermal conductivity. *Exp Therm Fluid Sci* 2009; 33: 922–928.
24. Shahil KM and Balandin AA. Graphene-multilayer graphene nanocomposites as highly efficient thermal interface materials. *Nano Lett* 2012; 12: 861–867.
25. Song N-J, Chen C-M, Lu C, et al. Thermally reduced graphene oxide films as flexible lateral heat spreaders. *J Mater Chem A* 2014; 2: 16563–16568.
26. Botas C, Álvarez P, Blanco C, et al. Critical temperatures in the synthesis of graphene-like materials by thermal exfoliation–reduction of graphite oxide. *Carbon* 2013; 52: 476–485.
27. McAllister MJ, Li J-L, Adamson DH, et al. Single sheet functionalized graphene by oxidation and thermal expansion of graphite. *Chem Mater* 2007; 19: 4396–4404.
28. Nethravathi C and Rajamathi M. Chemically modified graphene sheets produced by the solvothermal reduction of colloidal dispersions of graphite oxide. *Carbon* 2008; 46: 1994–1998.
29. Hirata M, Gotou T, Horiuchi S, et al. Thin-film particles of graphite oxide 1: High-yield synthesis and flexibility of the particles. *Carbon* 2004; 42: 2929–2937.
30. Marcano DC, Kosynkin DV, Berlin JM, et al. Improved synthesis of graphene oxide. *ACS Nano* 2010; 4: 4806–4814.
31. Hummers WS and Offeman RE. Preparation of graphitic oxide. *J Am Chem Soc* 1958; 80: 1339.
32. D'Agostino AT. Determination of thin metal film thickness by X-ray diffractometry using the Scherrer equation, atomic absorption analysis and transmission/reflection visible spectroscopy. *Anal Chim Acta* 1992; 262: 269–275.
33. Pope CG. X-ray diffraction and the Bragg equation. *J Chem Educ* 1997; 74: 129–131.
34. Shenogin S, Bodapati A, Xue L, et al. Effect of chemical functionalization on thermal transport of carbon nanotube composites. *Appl Phys Lett* 2004; 85: 2229–2231.
35. Hopkins PE. Multiple phonon processes contributing to inelastic scattering during thermal boundary conductance at solid interfaces. *J Appl Phys* 2009; 106: 013528–013529.
36. Ye Z-Q, Cao B-Y, Yao W-J, et al. Spectral phonon thermal properties in graphene nanoribbons. *Carbon* 2015; 93: 915–923.
37. Roy N, Sengupta R and Bhowmick AK. Modifications of carbon for polymer composites and nanocomposites. *Progr Polym Sci* 2012; 37: 781–819.
38. Hu GJ and Cao BY. Thermal resistance between crossed carbon nanotubes: Molecular dynamics simulations and analytical modeling. *J Appl Phys* 2013; 114: 224308–224308-224308.
39. Agari Y and Uno T. Thermal conductivity of polymer filled with carbon materials: Effect of conductive particle chains on thermal conductivity. *J Appl Polym Sci* 1985; 30: 2225–2235.